Synergy-based Optimal Sensing Techniques for Hand Pose Reconstruction

Matteo Bianchi, Paolo Salaris and Antonio Bicchi

Abstract Most of the neuroscientific results on synergies and their technical implementations in robotic systems, which are widely discussed throughout this book (see e.g. Chapters 1, 2, 3, 7, 9, 11 and 12), moved from the analysis of hand kinematics in free motion or during the interaction with the external environment. This observation motivates both the need for the development of suitable and manageable models for kinematic recordings, as described in Chapter 13, and the calling for accurate and economic systems or "gloves" able to provide reliable hand pose reconstructions. However, this latter aspect, which represents a challenging point also for many human-machine applications, is hardly achievable in economically and ergonomically viable sensing gloves, which are often imprecise and limited. To overcome these limitations, in this Chapter we propose to exploit the bi-directional relationship between neuroscience and robotic/artificial systems, showing how the findings achieved in one field can inspire and be used to advance the state of art in the other one, and vice versa. More specifically, our leading approach is to use the concept of kinematic synergies to optimally estimate the posture of a human hand using non-ideal sensing gloves. Our strategy is to collect and organize synergistic information and to fuse it with insufficient and inaccurate glove measurements in a consistent manner and with no extra costs. Furthermore, we will push forward such an analysis to the dual problem of how to design pose sensing devices, i.e. how

Matteo Bianchi
Department of Advanced Robotics (ADVR) – Istituto Italiano di Tecnologia, via Morego 30, 1613 Genova, Italy and Research Centre "E.Piaggio" – Università di Pisa, Largo Lucio Lazzarino 1, 56126 Pisa, Italy, e-mail: matteo.bianchi@iit.it

Paolo Salaris
Laboratoire d'analyse et d'architecture des systèmes (LAAS) – CNRS, avenue du Colonel Roche, 7, BP 54200 31031 Toulouse cedex 4, France, e-mail: salarispaolo@gmail.com

Antonio Bicchi
Research Centre "E.Piaggio" – Università di Pisa, Largo Lucio Lazzarino 1, 56126 Pisa, Italy and Department of Advanced Robotics (ADVR) – Istituto Italiano di Tecnologia, via Morego 30, 1613 Genova, Italy, e-mail: bicchi@centropiaggio.unipi.it

and where to place sensors on a glove, to get maximum information about the actual hand posture, especially with a limited number of sensors. We will study the optimal design of gloves of different nature. Conclusions that can be drawn take inspiration from and might inspire further investigations on the biology of human hand receptors. Experimental evaluations of these techniques are reported and discussed.

1 Introduction

The problem to achieve a correct and reliable hand pose estimation through Hand Pose Reconstruction (HPR) systems or "gloves" ([12, 34]) has gained an increasing importance for human-machine interactions in numerous applications such as robotics, rehabilitation, virtual reality and motion analysis. Furthermore, the study of human hand in psychophysical and neuroscientific studies requires accurate biomechanic and postural measurements together with refined kinematic models [18] to test and analyze theoretical motion control hypotheses [29], as it is widely discussed e.g. in Chapters 1, 2, 3 and 13.

Unfortunately, all current HPR methods are limited due to non - idealities, such as an imperfectly known relationship between the measurements and the complexity of the mechanical Degrees of Freedom (DoFs) of the human hand as well as considerations that tend to discourage the usage of many sensors. Regarding this last point, economic motivations are crucial to determine the choice of both the technology solution in use and the number of sensing elements. Under this regard, a meaningful example is the CyberGlove (CyberGlove System LLC, San Jose, CA – USA), which is one of the most popular HPR glove-based systems: such a glove can come equipped with 18 or 22 piezoresistive sensors but its overall cost grows from 12,297 USD to 17,795 USD (2010 quotes). On the other side, the need of enabling mass diffusion has led to the development of more economic but inaccurate devices: e.g. Mattel's PowerGlove (Mattel Inc., El Segundo, CA–USA), which usually met with scarce acceptance due to their imprecision. Ideally, the goal is to have systems that are economic but effective.

This Chapter, which is based on [1, 3], gives a global vision of the twofold problem of (i) optimally estimating human hand posture from partial and noisy HPR data – hence improving their accuracy at no extra costs – and (ii) how to optimally design pose sensing devices, i.e. how and where to place sensors on the human hand, to get maximum information about the actual hand pose despite limitations on their number and capabilities. This last point can be inspired from and offers interesting insights into biological investigations on human mechanoreceptors, as it will be discussed later in Section 2. Such a bi-directional relationship between natural and artificial side will be deeply analyzed in this Chapter, representing the *leitmotif* of this work and all this book.

Indeed, the leading idea of our approach is the concept of "human hand synergies" [29, 30, 31] (see also Chapters 1 - 5, 7, 9, 11 and 12): i.e. although very complex and possibly different in size and shape, human hands share many com-

monalities in how they are shaped and used in frequent everyday tasks. We will exploit such an information on the most frequent and probable hand postures to advance the state of art of hand sensing systems and robotics and, at the same time, to provide technical and theoretical tools to improve neuroscientific knowledge on human hand, in a mutual inspiration between biology and artificial sciences.

2 Biology and Artificial Systems: a Mutual Inspiration

As deeply discussed throughout this book, in recent years numerous studies have inquired in how the brain can organize the huge sensory – motor complexity of the human hand, with particular reference to grasping. One of the main findings is that there is a reduced number of coordination patterns, or *synergies*, related to both biomechanical [15] and neural factors [22], which correlate both joint motions and force exertions of multiple fingers [31] (see Chapters 1 - 5, 7 - 12). Multivariate statistical methods over a grasping data set also revealed that a limited amount of so–called *principal components* (or *eigenpostures* [25] [1]) can explain a great part of hand pose kinematic variability [29]. All these results suggest that it is possible to reduce the number of DoFs to be used according to a desired level of approximation.

Such an idea has been extensively used in robotics from a *controllability* point of view to define simplified strategies for the design and control of artificial hands [8, 9, 17] as it is discussed in Chapter 7. However, synergy concept can be also profitably exploited from the *observability* point of view, i.e. how to reduce the number of independent DoFs to be measured in order to obtain reliable hand pose estimations (cf. [26] for an application in hand avatar animation). Indeed, if the human hand moves according to patterns of most frequent use, it could be possible to exploit this information to improve hand pose reconstruction despite measurements, which are in general noisy and reduced in number. This observation suggests a strong relationship between sensory and motor side, which lays the foundations of the concept we defined as *sensory-motor synergies*, as discussed in Chapter 4 and in particular in Chapter 6.

In this Chapter we will deal with such an observability problem. More specifically, in the first part we will provide Minimum Variance Estimation techniques to fuse synergistic kinematic information with partial and noisy glove measurements. In the second part, we will push forward such an analysis, wondering: "and if I were the designer, how could I choose and place the sensors on a glove to maximize hand postural information?".

This last question is extremely important since it further reveals deep relationships between the artificial and natural side. Indeed, that the optimal distribution of sensitivity for HPR is not trivial is strongly suggested by the observation of the human example. Let us consider the role of cutaneous information and its relationship with proprioception and kinaesthesia of human hands and fingers, as it was investi-

---

[1] Hereinafter, in this Chapter the terms *synergies* and *principal components* will be used as synonyms.

(a) Slowly adapting (SA) units location.

(b) Fast adapting (FA) units location.

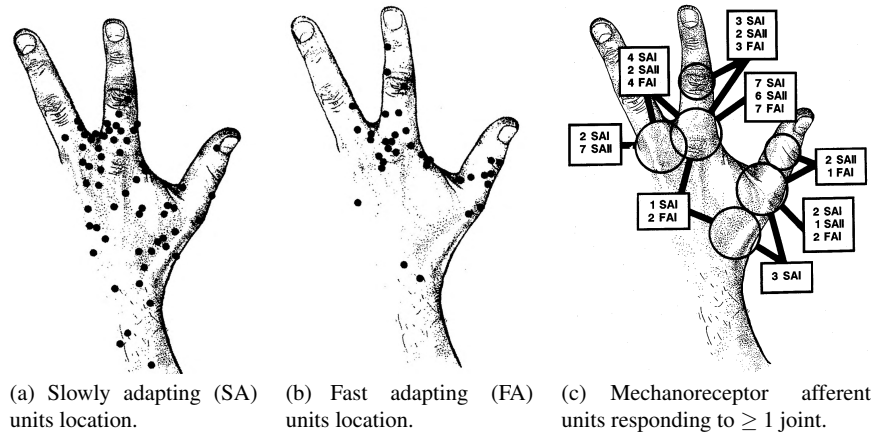(c) Mechanoreceptor afferent units responding to ≥ 1 joint.

Fig. 1 Location of cutaneous mechanoreceptive units in the dorsal skin of the human hand. Adapted from [13], courtesy of the authors.

gated in [13] where the response to finger movements of cutaneous mechanoreceptors in the dorsal skin of human hand was studied. Two main classes of mechanoreceptors involved in this response were roughly identified: Fast Adapting afferents of the first type (FAI), and Slow Adapting afferents, of both the first and second type (SAI and SAII, respectively). These two classes have non–uniform distributions as it is shown in figure 1(a) and 1(b). Indeed, FA units, which have a more localized response to movements about one or, at most, two nearby joints, are primarily close to joints, while SA units, which respond to several joints at the same time, can be found more uniformly distributed (see figure 1(c)).

Conclusions that can be drawn suggest that in the human hand sensory system there are different typologies of proprioceptive sensors on the skin with different distributions and densities, thus producing a non–uniform map of sensitivities to joint angles. Nonetheless the functional motivations of these data is still unclear, a fascinating interpretation might be the different importance of different elementary percepts in building an overall representation of the hand pose. These biological results motivate our approach to deal with the problem of searching for a preferential distribution and density of different typologies of sensors, which optimize the accuracy of glove–based HPR systems, especially when restrictions on the production costs limit both the number and the quality of sensors. As kinematic synergies is the leading idea for our optimal estimation approach and, together with the observations on the biology of human mechanoreceptors, the motivation for the optimal design of hand pose sensing systems, results we have achieved on the artificial side might further inspire biological investigations, providing theoretical and technical tools to advance the study of human hand sensory – motor apparatus.

3 Performance Enhancement

The approach we propose to improve the reconstruction accuracy of existing sensing gloves can deal with noisy measured data and relies on classic *Minimum Variance Estimation* (MVE). To validate this technique, we used a set of grasp postures acquired with a low cost sensing glove, which provides few noisy measurements, and an optical tracking system, which represents the accurate ground – truth for pose reconstruction.

3.1 The Hand Posture Estimation Algorithm

Let us consider a set of measures $y \in \mathbb{R}^m$ given by a sensing glove. By using a n degree of freedom kinematic hand model, let us assume a linear relationship between joint variables $x \in \mathbb{R}^n$ and measurements y given by

$$y = Hx + v, \tag{1}$$

where $H \in \mathbb{R}^{m \times n}$ ($m < n$) is a full rank matrix, which represents the relation between measures and joint angles, and $v \in \mathbb{R}^m$ is a vector of measurement noise. The goal is to determine the hand posture, i.e. the joint angles x, by using a set of measures y whose number is lower than the number of DoFs describing the kinematic hand model in use. As a consequence, (1) represents a system where there are fewer equations than unknowns and hence is compatible with an infinite number of solutions, described e.g. as

$$x = H^{\dagger} y + N_h \xi, \tag{2}$$

where $H^{\dagger}$ is the pseudo-inverse of matrix H, N_h is the null space basis of matrix H and $\xi \in \mathbb{R}^{(n-m)}$ is a free vector of parameters. Among these possible solutions, the least-squared solution resulting from the pseudo-inverse of matrix H for system (1) (hereianfter referred to as Pinv) is a vector of minimum Euclidean norm given by

$$\hat{x} = H^{\dagger} y. \tag{3}$$

However, the hand pose reconstruction resulting from (3) can be very far from the real one. The goal is to improve the accuracy of the pose reconstruction, choosing, among the possible solutions to (2), the most likely hand pose, taking into account the fact that finger motions in grasping tasks are strongly correlated according to some coordination patterns, or synergies [29] (cf. Section 2 and Chapters 1, 2 and 7).

To achieve this goal, we use as *a priori* information the synergistic information obtained by collecting a large number N of grasp postures x_i with n DoFs into a matrix $X \in \mathbb{R}^{n \times N}$. This information can be summarized by means of a covariance matrix $P_o \in \mathbb{R}^{n \times n}$, which is a symmetric matrix computed as $P_o = \frac{(X - \bar{x})(X - \bar{x})^T}{N - 1}$, where $\bar{x}$ is a matrix $n \times N$ whose columns contain the mean values for each joint angle ar-

ranged in vector $\mu_o \in \mathbb{R}^n$. We assume that the above described *a priori* information is multivariate normal distributed, and hence can be described by the covariance matrix P_o.

3.1.1 Minimum Variance Estimation

Minimum Variance Estimation (MVE) technique minimizes a cost functional that expresses the weighted Euclidean norm of deviations, i.e. cost functional $J = \int_X (\hat{x}-x)^T S(\hat{x}-x)dx$, where S is an arbitrary, semidefinite positive matrix. Under the hypothesis that v has zero mean and Gaussian distribution with covariance matrix R, the solution for the minimization of J is achieved as $\hat{x} = E[x|y]$, where $E[x|y]$ represents the *a posteriori* probability density function (pdf) expectation value of the multivariate normal distribution. This function is expressed by [35] as

$$f(x) = \frac{1}{\sqrt{2\pi\|P_o\|}} \exp\left\{-\frac{1}{2}(x-\mu_o)^T P_o^{-1}(x-\mu_o)\right\}. \tag{4}$$

The estimation $\hat{x}$ can be obtained as in [19] by

$$\hat{x} = (P_o^{-1}+H^T R^{-1}H)^{-1}(H^T R^{-1}y+P_o^{-1}\mu_o), \tag{5}$$

where matrix $P_p = (P_o^{-1}+H^T R^{-1}H)^{-1}$ is the *a posteriori* covariance matrix, which has to be minimized to increase information about the system. This result represents a very common procedure in applied optimal estimation when there is redundant sensor information. In under-determined problems, it is only thanks to the *a priori* information, represented by P_o and μ_o, that equation (5) can be applied (indeed, $H^T R^{-1}H$ is not invertible).

When R tends to assume very small values, the solution described in equation (5) might encounter numerical problems. However, by using the Sherman-Morrison-Woodbury formulae,

$$(P_o^{-1}+H^T R^{-1}H)^{-1} = P_o - P_o H^T (HP_o H^T +R)^{-1}HP_o \tag{6}$$
$$(P_o^{-1}+H^T R^{-1}H)^{-1}H^T R^{-1} = P_o H^T (HP_o H^T +R)^{-1}, \tag{7}$$

equation (5) can be rewritten as

$$\hat{x} = \mu_o - P_o H^T (HP_o H^T +R)^{-1}(H\mu_o - y), \tag{8}$$

and the *a posteriori* covariance matrix becomes $P_p = P_o - P_o H^T (HP_o H^T +R)^{-1}HP_o$. By placing $R = 0$ in (8), it is possible to obtain equation (7) and the *a posteriori* covariance matrix becomes

$$P_p = P_o - P_o H^T (HP_o H^T)^{-1}HP_o \tag{9}$$

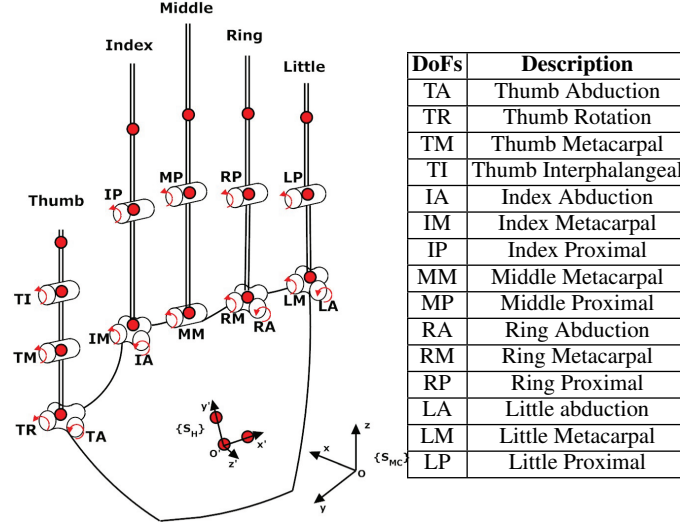| DoFs	Description
TA	Thumb Abduction
TR	Thumb Rotation
TM	Thumb Metacarpal
TI	Thumb Interphalangeal
IA	Index Abduction
IM	Index Metacarpal
IP	Index Proximal
MM	Middle Metacarpal
MP	Middle Proximal
RA	Ring Abduction
RM	Ring Metacarpal
RP	Ring Proximal
LA	Little abduction
LM	Little Metacarpal
LP	Little Proximal

Fig. 2 Kinematic model of the hand with 15 DoFs. Markers are reported as red spheres.

Notice that, (8) with $R = 0$ can also be obtained by maximizing the pdf (4), that is equivalent to solving the following optimal control problem (see [4] for details):

$$\begin{cases} \hat{x} = \underset{\hat{x}}{\arg\min} \ \frac{1}{2}(x - \mu_o)^T P_o^{-1}(x - \mu_o) \\ \text{Subject to} \quad y = Hx. \end{cases} \tag{10}$$

It is interesting to give a geometrical interpretation of the cost function in (10), which expresses the square of the Mahalanobis distance [24]. The concept of Mahalanobis distance, which takes into account data covariance structure, is widely exploited in statistics, e.g. in Principal Components Analysis, mainly for outlier detection [21]. Accordingly, to assess if a test point belongs to a known data set, whose distribution defines an hyper-ellipsoid, its closeness to the centroid of data set is taken into account as well as the direction of the test point w.r.t. the centroid itself. In other words, the more samples are distributed along a given direction, the higher is the probability that the test point belongs to the data set even if it is further from the center.

Fig. 3 The sensing glove used in our study (on the left) and the sensing glove with added markers (on the right).

3.2 Data Acquisition

To assess hand pose reconstruction effectiveness, without loss of generality, we used a 15 DoF model for the hand[2], which was also considered in [17, 29] and reported in Fig. 2. We collected a large number of static grasp positions using 19 active markers and an optical motion capture system (Phase Space, San Leandro, CA, USA). More specifically, all the grasps of the 57 imagined objects described in [29] were performed twice by subject AT (M,26), in order to define a set of 114 *a priori* data. We characterized such an *a priori* information in terms of P_o and μ_o.

Moreover, 54 grasp poses of a wide range of different imagined objects were executed by subject LC (M,26) [3]. The set of the latter poses will be referred hereinafter as *validation set*, since these poses can be assumed to represent accurate reference angular values for successive comparisons with the obtained hand pose reconstructions. For this reason, these data were recorded in parallel with the sensing glove, whose performance we wanted to optimize, as it will be described later in this Section, and the Phase Space system, in order to achieve also glove calibration. The processed hand poses acquired with Phase Space can be considered as reliable approximations of real hand positions, given the high accuracy provided by this optical system to detect markers (the amount of static marker jitter is inferior than 0.5 mm, usually 0.1 mm) and assuming a linear correlation (due to skin stretch) between marker motion around the axes of rotation of the joint and the movement of the joint itself [40]. Since the sensing glove perfectly adapts to subject hand shape when it is worn, the latter assumption is still reasonable also in this case, even if departures from real reference configurations can happen. None of the subjects had physical limitations that would affect the experimental outcomes. Data collection from subjects in this study was approved by the University of Pisa Institutional Review Board. For the markerization protocol and additional details on the acquisition, the reader is invited to refer to [1].

---

[2] The human hand, considering only fingers and metacarpal joints, has 23 DoFs [12]. Various models have been proposed in literature, which try to reproduce hand and wrist kinematics at different levels of approximation, e.g. [16, 18, 33]

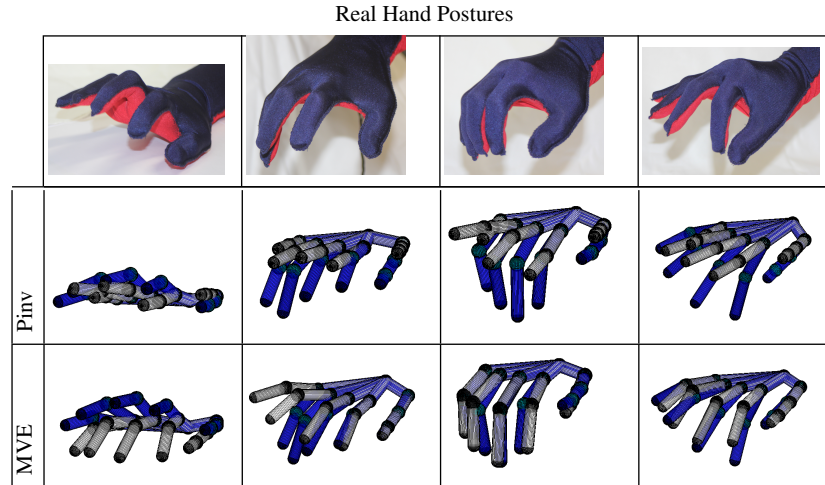[3] All these data and more information about hand pose acquisitions are available at http://handcorpus.org/

Real Hand Postures

Fig. 4 Hand pose reconstructions with Pinv and MVE algorithms, with measures given by the sensing glove. In blue the "real" hand posture whereas in white the estimated one.

3.3 Experimental Results
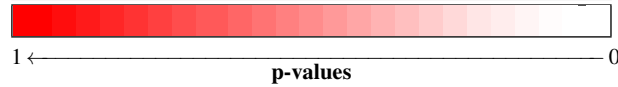
The reconstruction procedure was tested using a sensorized glove based on Conductive Elastomer (CE) [36]. CE strips are printed on a Lycra®/cotton fabric in order to follow the contour of the hand, see Fig. 3.

Since CE materials present piezo-resistive characteristics, sensor elements corresponding to different segments of the contour of the hand length change as the hand moves. These movements cause variations in the electrical properties of the material, which can be revealed by reading the voltage drop across such segments.The sensors are connected in series thus forming a single sensor line while the connections intersect the sensor line in the appropriate points.

In the present study, long finger flexion-extension recognition was obtained by means of an updated multi-regressive model having the metacarpophalangeal (MCP) flexion-extension angles of the five long fingers as dependent variables and the outputs of CE sensor covering MCP joints as independent ones. According to the hand kinematic model adopted in this work they are referred as to TM, IM, MM, RM, LM. The model parameters were identified by measuring the sensor status in two different position: (1) hand totally closed (90 degrees), (2) hand totally opened (0 degrees). For more information about the design and structure of the here described sensing glove and the signal processing system employed, the reader is invited to refer to [23, 36, 37].

Although this sensorized glove can be regarded as one of the most recent and inexpensive envisions in glove device literature, it is limited under several aspects that can reduce its performance, e.g cloth support that affects measurement repeatability

DoF	Mean±Std		Max Error		p-values
	MVE	**Pinv**	**MVE**	**Pinv**	
TA	12.12±9.98	14.37±10.78	36.63	34.28	**0.28**
TR	9.20±7.13	26.46±10.49	26.34	46.43	0
TM∗	4.36±3.73	6.43±4.44	13.25	18.50	0.0093
TI	14.56±9.96	7.84±5.47	33.25	22.38	0.0008
IA	9.82±6.89	7.10±5.08	29.60	21.18	0.0381
IM∗	15.27±11.86	16.48±12.62	46.76	43.58	**0.58**
IP	9.60±7.65	31.47±14.70	27.40	61.11	0
MM∗	14.40±12.84	19.88±14.58	53.03	51.47	0.0232
MP	6.80±6.49	24.36±9.85	24.74	43.72	0
RA	6.20±4.31	5.69±4.72	15.72	20.90	**0.51**
RM∗	19.00±13.44	19.22±11.81	61.98	46.32	**0.67**
RP	8.98±8.91	31.51±13.98	32.24	60.62	0
LA	11.42±8.50	32.24±6.98	29.59	48.11	0
LM∗	17.37±12.51	17.98±11.81	58.40	45.05	**0.26**
LP	8.43±6.36	23.90±12.53	26.07	56.21	0

$1 \longleftarrow$ **p-values** $\longrightarrow 0$

∗ indicates a measured DoF.

Table 1 Average estimation errors and standard deviations for each DoF [°], for the sensing glove acquisitions. MVE and Pinv methods are considered. Maximum errors are also reported as well as p-values from the evaluation of DoF estimation errors between MVE and Pinv. A color map describing p-values is also added to simplify result visualization. ⋄ indicates that standard two-tailed t-test (T_{eq}) is exploited for the comparison. ‡ indicates a modified two-tailed T-test (Behrens-Fisher problem), T_{neq} test. When no symbol appears near the tabulated values, it means that Mann-Whitney U-test (U-test) is used. **Bold** value indicates no statistical difference between the two methods under analysis at 5% significance level. When the difference is significative, values are reported with a 10^{-4} precision. p-values less than 10^{-4} are considered equal to zero.

as well as hysteresis and non linearities due to piezo-resistive material properties. Indeed, although this kind of glove is suitable for general opening/closening hand movement measurement, it is not the best choice for sensing fine hand adjustments. Moreover, the assumptions done for data processing (the relationship between joint angles and sensors as well as the linearity between hand aperture and electrical property changes) and the calibration phase based only on two-points fitting can act like aditional potential sources of errors. To overcome this last point we performed a new calibration to estimate the measurement matrix.

3.3.1 Results and Discussions

First, we obtained an estimation of the glove measurement matrix H_g, i.e. $\hat{H}_g$. For this purpose, a calibration phase was performed by collecting a number of poses

N in parallel with the glove and the position optical tracking system. This number has to be larger or equal than the dimension of the state to estimate, i.e. $N \geq 15$. $X_c \in \mathbb{R}^{15 \times 15}$ collects the reference poses, while matrix $Z_c \in \mathbb{R}^{5 \times 15}$ organizes the measures from the glove. These measures represent the values of the signals referred to measured joints veraged over the last 50 acquired samples (@250 kS/s). Matrix $\hat{H}_g$ can be obtained by exploiting the relation $Z_c = \hat{H}_g X_c$ as $\hat{H}_g = Z_c ((X_c^T)^\dagger)^T$. Measurement noise was characterized in terms of fluctuations w.r.t. the aforementioned average values of the measures, thus obtaining noise covariance matrix R. Noise level is less than 10% measurement amplitude. However consistent errors in the measurement matrix estimation might be obtained due to intrinsic non-linearities and hysteresis of glove sensing elements. Once the measurement matrix $\hat{H}_g$ was obtained, we applied MVE estimation techniques to the measurements provided by the glove and compared the results with those achieved using simple pseudo-inversion (Pinv) (2).

Pose estimation errors (i.e. the mean of DoF absolute estimation errors computed for each pose $e_i = \frac{1}{n} \sum_{i=1}^{n} |x_i - \hat{x}_i|$), and DoF absolute estimation errors are considered and averaged over all the number of reconstructed poses.

Results clearly show that MVE outperforms Pinv in terms of estimation outcomes. Indeed, the average absolute pose estimation error with MVE is $10.94 \pm 4.24°$, while it is equal to $19.00 \pm 3.66°$ by using Pinv. Statistical difference was observed between the two techniques (p-value less than 10^{-4}). Notice that MVE exhibits best pose reconstruction performances also in terms of maximum errors ($25.18°$ for MVE vs. $30.30°$ for Pinv). Absolute average reconstruction errors for each DoF are reported in table 1. MVE produces the best results which are statistically different w.r.t. Pinv algorithm, see table 1, except, respectively, for those DoFs which are directly measured (i.e. IM, RM and LM), for RA DoF, which exhibits a limited average estimation error ($\approx 6°$), and finally TA. For TI the smallest average estimation is observed with Pinv; a possible explanation for this might be still related to the difficulties in kinematic modeling thumb phalanx kinematics. IA DoF presents the smallest absolute average estimation error with Pinv, although p-values from the comparisons between the two techniques for the estimation of this DoF are close to the significance threshold. Maximum DoF reconstruction errors for MVE are observed especially for those measured DoFs with potentially maximum variations in grasping tasks; this fact may be probably due to the non linearities in sensing glove elements leading to inaccurate estimation of H_g, and hence to inaccurate measures. Furthermore, MVE aims at minimizing the error statistics and guarantees that the mean squared norm of the joint error vector (i.e. the Mean Squared Error, $MSE = \frac{1}{N} \sum_{i=1}^{N} \|\hat{x} - x\|^2$, where N represents the number of predictions) is minimized, but not necessarily the value of each single component. For this reason, some worst-case sensing results can be found.

To conclude, except for some singular poses, the best estimation performance is provided by MVE for which a good robustness to errors in measurement process modeling is also observed. However, the latter errors are not taken numerically into account in these analyses. Moreover, as it can been seen in Fig. 4, reconstructed hand

configurations obtained by MVE preserve likelihood with real poses, as opposed to pseudo-inverse based algorithm.

4 Optimal Design

In this part of the Chapter, we extend the analysis to the optimal design of sensing gloves. The objective is to choose the optimal sensor distribution that maximizes the information on the actual posture. This information, used with the estimation method previously discussed, will lead to the minimization of the reconstruction error statistics.

As explained in Section 2, there is a strong biological evidence that the optimal distribution of sensitivity for a sensing glove should not be trivial. However, while most results in optimal experimental design [6, 10, 20] refer to the case where the number of measurements is redundant or at least equal to the number of variables to be estimated, the opposite case that fewer sensors are available than the hand variables is of main concern in our problem. To circumvent this limit, it is natural to think of exploiting synergistic *a priori* knowledge to disambiguate poses from scarce data.

In previous sections, synergistic prior knowledge on how humans most frequently use their hands is fused with partial and noisy data provided by any given glove device, to maximize reconstruction accuracy. Here, the goal is to characterize a design that enables for optimally exploiting – in a Bayesian sense – such an *a priori* information.

The optimization goals become particularly relevant when restrictions on the production costs limit both the number and the quality of sensors. In these cases, a careful design is instrumental to obtain good performance. Furthermore, different technologies and sensor distributions can be considered to realize the devices. At the physical level, sensors for gloves can be classified as either *lumped* (as e.g. a mechanical angular encoder about a joint or Hall-effect sensors, as in the Humanglove by Humanware s.r.l. (Pisa, Italy)) or *distributed* (e.g. a flexible optic fiber running along a finger from base to tip or conductive elastomeric strips as in the glove used in our experiments [36]). At the signal level, glove sensors can be *coupled* (if more than one hand joint angle influences the reading) or *uncoupled*. Of course, all distributed sensors are coupled, but also lumped sensors can exhibit cross–coupling.

Different sensor arrangements generate different measurement matrices H: the row corresponding to a lumped, uncoupled sensor has a non–zero element only in correspondence to the measured joint, hence (up to rescaling) it is a binary "selection" matrix. We will call such a matrix *discrete*, i.e. $H_{ij} \in \{0, 1\}$ — a *discrete* set of values. Conversely, a coupled sensor with general weights, i.e. a distributed sensor or a lumped sensor with not negligible cross–coupling, produces a matrix whose row elements are real numbers, i.e., up to rescaling, $H_{ij} \in [-1, 1] \subset \mathbb{R}$ — a *continuous* set of values. In the following, we will call such a matrix *continuous*. Finally, a glove employing both lumped (uncoupled and coupled) and distributed sensors will

generate a *hybrid* measurement matrix, which consists of a continuous part and a discrete one.

Lumped, uncoupled sensing devices, which generate a discrete measurement matrix, are probably the easiest to be implemented, as they require to individually measure single joints according to the optimal measurement matrix. Common sensing strategies include Hall–effect or piezoresistive sensors (e.g. CyberGlove, by Cyber-Glove System LLC), directly placed on the joints to be measured, hence obtaining a lumped device. On the other hand, distributed sensors, which generate an optimal continuous matrix like the sensing glove used in the experiments described in Section 3.3, should provide measurements in terms of (optimally) weighted linear combinations of the contributions of different DoFs, e.g. using, among the different techniques, resistive ink printed on flexible plastic bends that follow the movement of hand joints (e.g. PowerGlove by Mattel Inc., El Segundo, CA–USA), or capacitive sensors (as e.g. in the Didjiglove by Dijiglove Pty. Ltd., Melbourne, AUS) [12]. Finally, the above discussed technologies (lumped, uncoupled and distributed) can be adopted and combined in an efficient manner to optimally realize devices that can be modeled by a hybrid measurement matrix. Notice that the human hand sensing distribution can be considered to belong to the latter glove class, as it will be discussed later in this Chapter.

4.1 Problem Definition

In the ideal case of noiseless measures ($R = 0$), P_p becomes zero when H is a full rank n matrix, meaning that the available measures contain a complete information about the hand posture. In the real case of noisy measures and/or when the number of measurements m is less than the number of DoFs n, P_p can not be zero. In these cases, the following problem becomes very interesting: find the optimal matrix H^* such that the hand posture information contained in a reduced number of measurements is maximized. Without loss of generality, let assume H to be full row rank and consider the following problem.

Problem 1. Let H be an $m \times n$ full row rank matrix with $m < n$ and $V_1(P_o, H, R) : \mathbb{R}^{m \times n} \to \mathbb{R}$ be defined as $V_1(P_o, H, R) = \|P_o - P_o H^T (H P_o H^T + R)^{-1} H P_o\|_F^2$, find

$$H^* = \arg\min_H V_1(P_o, H, R)$$

where $\|\cdot\|_F$ denotes the Frobenius norm defined as $\|A\|_F = \sqrt{\mathrm{tr}(A A^T)}$, for $A \in \mathbb{R}^{n \times n}$.

Frobenius norm has been already used in literature for optimization in measurement problem, e.g. [27]. Here the squared Frobenius norm is adopted to exploit its useful relation with matrix trace operator in order to simplify the derivation of the matrix gradient flow later defined. To solve problem 1 means to minimize the entries of the *a posteriori* covariance matrix: the smaller the values of the elements in P_p,

the greater is the predictive efficiency. Next sections will be dedicated to describe solutions to problem 1 for different sensor distributions and hence measurement matrices, i.e. continuous, discrete and hybrid, the latter containing both lumped and distributed sensors.

Let us introduce some useful notations. If M is a symmetric matrix with dimension n, let its Singular Value Decomposition (SVD) be $M = U_M \Sigma_M U_M^T$, where Σ_M is the diagonal matrix containing the singular values $\sigma_1(M) \geq \sigma_2(M) \geq \cdots \geq \sigma_n(M)$ of M and U_M is an orthogonal matrix whose columns $u_i(M)$ are the eigenvectors of M, known as Principal Components (PCs) of M, associated with $\sigma_i(M)$. For example, the SVD of the *a priori* covariance matrix is $P_o = U_{P_o} \Sigma_{P_o} U_{P_o}^T$, with $\sigma_i(P_o)$ and $u_i(P_o)$, $i = 1, 2, \ldots, n$, the singular values and the principal components of matrix P_o, respectively.

4.2 Continuous Sensing Design

In this case, each row of matrix H is a vector in $\mathbb{R}^n$ and hence can be given as a linear combination of a $\mathbb{R}^n$ basis. Without loss of generality, we can use the principal components of matrix P_o, i.e. columns of previously defined matrix U_{P_o}, as a basis of $\mathbb{R}^n$. Consequently, naming H_c such a type of matrix related to a continuous sensing device, the measurement matrix can be written as $H_c = H_e U_{P_o}^T$, where $H_e \in \mathbb{R}^{m \times n}$ contains the coefficients of the linear combinations. Given that $P_o = U_{P_o} \Sigma_{P_o} U_{P_o}^T$, the *a posteriori* covariance matrix becomes

$$P_p = U \left[\Sigma_o - \Sigma_o H_e^T (H_e \Sigma_o H_e^T + R)^{-1} H_e \Sigma_o \right] U^T, \tag{11}$$

where, for simplicity of notation $\Sigma_o \equiv \Sigma_{P_o}$.

We will analyze the optimal continuous sensing design both under a numerical and analytical point of view. For this purpose, let us introduce the set of $m \times n$ (with $m < n$) matrices with orthogonal rows, i.e. satisfying the condition $HH^T = I_{m \times m}$, and let denote it as $\mathcal{O}_{m \times n}$.

4.2.1 Numerical Solution: Gradient flows on $\mathcal{O}_{m \times n}$

A differential equation that solve problem 1 is proposed. The following proposition describes an algorithm that minimizes the cost function $V_1(P_o, H, R)$, providing the gradient flow which can be used to improve the method of steepest descent.

Proposition 1. *The gradient flow for the function $V_1(P_o, H, R) : \mathbb{R}^{m \times n} \to \mathbb{R}$ is given by,*

$$\dot{H} = -\nabla \|P_p\|_F^2 = 4 \left[P_p^2 P_o H^T \Sigma(H) \right]^T, \tag{12}$$

where $\Sigma(H) = (HP_oH^T + R)^{-1}$.

All the calculation to obtain the gradient can be found in the Appendix of [2].

Let us observe that rows of matrix H can be chosen, without loss of generality, such that $H_i P_o H_j^T = 0$, $i \neq j$ that imply that measures are uncorrelated, i.e. satisfying the condition $HH^T = I_m$. Of course, in case of noise-free sensors, this constraint is not strictly necessary. On the other hand, in case of noisy sensors, the minimum of $V_1(P_o, H, R)$ can not be obtained since it represents a limit case that can be achieved when H becomes very large (i.e. an infimum) and hence increasing the signal-to-noise ratio in an artificial manner. Therefore, it is possible to use the constraint $HH^T = I_m$ to reduce the search space in order to find solutions.

To solve this constrained problem it is possible to use the Rosen's gradient projection method for linear constraints [28], which is based on projecting the search direction into the subspace tangent to the constraint itself.

Having the search direction for the constrained problem, the gradient flow is given by

$$\dot{H} = -4W \left[P_p^2 P_o H^T \Sigma(H) \right]^T \tag{13}$$

where $\Sigma(H) = (H P_o H^T + R)^{-1}$. The gradient flow (12) guarantees that the optimal solution H^* will satisfy $H^*(H^*)^T = I_m$, if $H(0)$ satisfies $H(0)H(0)^T = I_m$, i.e. $H \in \mathcal{O}_{m \times n}$ [4].

Notice that both $\mathcal{O}_{m \times n}$ and $V_1(P_o, H, R)$ are not convex, hence the problem could not have a unique minimum. To overcome this common problem in gradient methods, a multi-start search represents a classic procedure. The here described gradient-based technique can be useful to characterize optimal solutions also for discrete sensing design, in case of large dimension problem. Moreover, they can furnish interesting suggestions about a possible hybrid approach later discussed.

4.2.2 Analytical Solutions

Let us first consider the case of noiseless measures, i.e. $R = 0$. Let A be a non-negative matrix of order n. It is well known (see [27]) that, for any given matrix B of rank m with $m \leq n$,

$$\min_B \|A - B\|_F^2 = \alpha_{m+1}^2 + \cdots + \alpha_n^2 \,, \tag{14}$$

where α_i are the eigenvalues of A, and the minimum is attained when

$$B = \alpha_1 w_1 w_1^T + \cdots + \alpha_m w_m w_m^T \,, \tag{15}$$

where w_i are the eigenvector of A associated with α_i. In other words, the choice of B as in (15) is the best fitting matrix of given rank m for A. By using this result we can determine when the minimum of (11), and hence of

$$\|\Sigma_o - \Sigma_o H_e^T (H_e \Sigma_o H_e^T)^{-1} H_e \Sigma_o\|_F^2 \,, \tag{16}$$

---

[4] $H(0)$ indicates the starting point at t = 0 for the gradient flow.

can be reached. Let us observe that the row vectors $(h_i)_e$ of H_e can be chosen, without loss of generality, to satisfy the condition $(h_i)_e \Sigma_o (h_j)_e = 0$, $i \neq j$, which implies that the measures are uncorrelated. As previously said, $\mathscr{O}_{m \times n}$ denotes the set of $m \times n$ matrices, with $m < n$, whose rows satisfy the aforementioned condition, i.e. the set of matrices with orthonormal rows ($H_e H_e^T = I$). By using (14), the minimum of (16) is obtained when (see [27])

$$\Sigma_o H_e^T (H_e \Sigma_o H_e^T)^{-1} H_e \Sigma_o = \sigma_1(\Sigma_o) u_1(\Sigma_o) u_1^T(\Sigma_o) + \cdots + \sigma_m(\Sigma_o) u_m(\Sigma_o) u_m^T(\Sigma_o). \tag{17}$$

Since Σ_o is a diagonal matrix, $u_i(\Sigma_o) \equiv e_i$, where e_i is the i-th element of the canonical basis. Hence, it is easy to verify that (17) holds for $H_e = [I_m \,|\, 0_{m \times (n-m)}]$. As a consequence, row vectors $(h_i)_c$ of H_c are the first m principal components of P_o, i.e. $(h_i)_c = u_i(P_o)^T$, for $i = 1, \ldots, m$.

From these results, a principal component can be defined as a linear combination of optimally-weighted observed variables meaning that the corresponding measures can account for the maximal amount of variance in the data set. As reported in [27], every set of m optimal measures can be considered as a representation of points in the best fitting lower dimensional subspace. Thus the first measure gives the best one dimensional representation of data set, the first two measures give the best two dimensional representation, and so on.

In case of noisy measures, (15) can not be verified since it represents a limit case that can be achieved when H becomes very large and hence increasing the signal-to-noise ratio. We hence describe an optimal solution for problem 1 in the set $\mathscr{A} = \{H : HH^T = I_m\}$. This problem was discussed and solved in [11], providing that, for arbitrarily noise covariance matrix R,

$$\min_{H \in \mathscr{A}} V_1(H) = \sum_{i=1}^{m} \frac{\sigma_i(P_o)}{1 + \sigma_i(P_o)/\sigma_{m-i+1}(R)} + \sum_{i=m+1}^{n} \sigma_i(P_o), \tag{18}$$

and it is attained for $H = \sum_{i=1}^{m} u_{m-i+1}(R) u_i(P_o)$.

Hence, if $\mathscr{A}$ consists of all matrices with mutually perpendicular, unit length rows, the first m principal components of P_o are always the optimal choice for H rows. As shown in [11] this situation changes under the Frobenius norm constraint, i.e. $\mathscr{A} = \{H : \|H\|_F \leq 1\}$ (see [11] for details).

Conclusions that can be drawn from this part is that in case of noise-free measures, the invariance of the cost function w.r.t. changes of basis, i.e. $V_1(P_o, H, 0) = V_1(P_o, MH, 0)$ with $M \in \mathbb{R}^m$ an invertible full rank matrix, suggests that there might exist a subspace in $\mathbb{R}^n$ where the optimum is achieved. Indeed, gradients become zero when rows of matrix H are any linear combination of a subset of m principal components of the *a priori* covariance matrix, or synergies [29]. Unfortunately, this does not happen in case of noisy measures and gradients become zero only for a particular matrix H which depends also on the principal components of the noise covariance matrix. In other terms, in case of continuous sensing gloves the sensing elements must be placed on the human hand in order to provide measurements that are related to the joints according to the first m PC weights.

4.3 Discrete Sensing Design

Let us consider now the case that each measure y_j, $j = 1, \ldots, m$ from the glove corresponds to a single joint angle x_i, $i = 1, \ldots, n$. The problem here is to find the optimal choice of m joints or DoFs to be measured.

Measurement matrix becomes in this case a full row rank matrix where each row is a vector of the canonical basis, i.e. matrices which have exactly one nonzero entry in each row: let H_d be such a type of matrix. The optimal choice H_d^* can be easily computed, by substituting all the possible sub-sets of m vectors of the canonical basis in the cost function $V_1(P_o, H, R)$. However, a more general approach to compute the optimal matrix is provided in order to obtain the solution also when a model with a large number of DoFs is considered, and eventually extended to all human body.

Let $\mathcal{N}_{m \times n}$ denote the set of $m \times n$ element-wise non-negative matrices, then $\mathscr{P}_{m \times n} = \mathscr{O}_{m \times n} \cap \mathcal{N}_{m \times n}$, where $\mathscr{P}_{m \times n}$ is the set of $m \times n$ permutation matrices (see lemma 2.5 in [39]). This result implies that if we restrict H to be orthonormal and element-wise non-negative, we get a permutation matrix. We extend this result in $\mathbb{R}^{m \times n}$, obtaining matrices which have exactly one nonzero entry in each row and the problem to solve becomes:

Problem 2. Let H be a $m \times n$ matrix with $m < n$, and $V_1(P_o, H, R) : \mathbb{R}^{m \times n} \to \mathbb{R}$ be defined as $V_1(P_o, H, R) = \|P_o - P_o H^T (H P_o H^T + R)^{-1} H P_o\|_F^2$, find the optimal measurement matrix

$$H^* = \arg\min_H V_1(P_o, H, R)$$

$$s.t. \quad H \in \mathscr{P}_{m \times n}.$$

4.3.1 Numerical Solution: Gradient Flows on $\mathscr{P}_{m \times n}$

A solution for this problem can be obtained defining a cost function that penalizes negative entries of H. In [39] authors defined a function $V_2(P)$ with $P \in \mathbb{R}^{n \times n}$ that forces the entries of P to be as "positive" as possible. In this Chapter, we extend this function to measurement matrices $H \in \mathbb{R}^{m \times n}$ with $m < n$ and hence, I consider a function $V_2 : \mathscr{O}_{m \times n} \to \mathbb{R}$ as

$$V_2(H) = \frac{2}{3} \mathrm{tr} \left[H^T (H - (H \circ H)) \right], \tag{19}$$

where $A \circ B$ denotes the *Hadamard* or elementwise product of the matrices $A = (a_{ij})$ and $B = (b_{ij})$, i.e. $A \circ B = (a_{ij} b_{ij})$. The gradient flow of $V_2(H)$ is given by [39]

$$\dot{H} = -H \left[(H \circ H)^T H - H^T (H \circ H) \right], \tag{20}$$

which minimizes $V_2(H)$ converging to a permutation matrix if $H(0) \in \mathscr{O}_{m \times n}$.

Up to this point, we have introduced two gradient flows given by (13) and (20), both on the space of orthogonal matrices, that respectively minimize their cost function, while the second one also converges to a permutation matrix. By combining these two gradient flows a solution for Problem 2 can be achieved. Of course, we can combine the gradient flows in two different ways: by adding them in a convex combination or firstly ignoring the non-negativity requirement and switching to the permutation gradient flow when the objective function has been sufficiently minimized [39].

Theorem 1. *Let $H \in \mathbb{R}^{m \times n}$ with $m < n$ the measurement process matrix and let me assume that $H(0) \in \mathcal{O}_{m \times n}$. Moreover, I suppose that $H(t)$ satisfies the following matrix differential equation,*

$$\dot{H} = 4\,(1-k)W\,\left[P_p^2 P_o H^T \Sigma(H)\right]^T + k\,H\left[(H \circ H)^T H - H^T (H \circ H)\right], \qquad (21)$$

where $k \in [0, 1]$ is a positive constant and $\Sigma(H) = (HP_oH^T + R)^{-1}$. For sufficiently large k (near one), $\lim_{t \to \infty} H(t) = H_\infty$ exists and approximates a permutation matrix that also minimizes the squared Frobenius norm of the a posteriori *covariance matrix, $\|P_p\|_F^2$.*

A proof for this theorem can be obtained directly by using results from [39] and further details can be found in [3].

4.4 Hybrid Sensing Design

In previous sections, optimal solutions for continuous and discrete sensing cases have been provided. However, in order to take advantage from both of them (the amount of information achievable vs low-cost implementation and feasibility) an hybrid sensing device which combines continuous and discrete sensors might represent a valid improvement, as it can be found also in biology. Indeed, human hand can be regarded – to some extent – as an example of hybrid sensory system. As previously discussed, among the cutaneous mechanoreceptors in the hand dorsal skin that were demonstrated to be involved in the responses to finger movements, and hence that possibly contribute to kinaesthesia, it is possible to find Fast Adapting (FA) type ones, which mainly respond to movements around one or at most two nearby joints and that can be regarded as "discrete" sensors, as well as the discharge rate of Slow Adapting (SA) afferents, which are influenced by several joints and can be regarded as "continuous" type sensors [14].

Up to re–arranging the sensor numbering, we can write a hybrid measurement matrix $H_{c,d} \in \mathbb{R}^{m \times n}$ as

$$H_{c,d} = \left[\begin{array}{c} H_c \\ \hline H_d \end{array}\right],$$

where $H_c \in \mathbb{R}^{m_c \times n}$ defines the m_c rows of the continuous part, whereas $H_d \in \mathscr{P}^{m_d \times n}$ describes the m_d single–joint measurements of the discrete part, with $m_c + m_d = m$. Neither the closed–form solution valid for the continuous measurement matrix, nor the exhaustion method used for discrete measurements are applicable in the hybrid case. Therefore, to optimally determine the hybrid measurement matrix, we will recur to gradient–based iterative optimization algorithms.

By combining the continuous and discrete gradient flows, previously defined in (12) and (20), respectively, and constraining the solution in the sub–set $\mathscr{H}_{c,d} = \{H_{c,d} : H_{c,d}H_{c,d}^T = I_m\}$, we obtain

$$
\dot{H}_{c,d} = 4\,(1-k)\,\left[P_p^2 P_o H_{c,d}^T \Sigma(H_{c,d})\right]^T\,W + k\,\bar{H}_d\left[(\bar{H}_d \circ \bar{H}_d)^T \bar{H}_d - \bar{H}_d^T(\bar{H}_d \circ \bar{H}_d)\right],
$$
(22)

where $k \in [0, 1]$ is a positive constant, $P_p = P_o - P_o H_{c,d}^T(H_{c,d}P_o H_{c,d}^T + R)^{-1}H_{c,d}P_o$, $W = I_n - H_{c,d}^T(H_{c,d}H_{c,d}^T)^{-1}H_{c,d}$, $\Sigma(H_{c,d}) = (H_{c,d}P_o H_{c,d}^T + R)^{-1}$, and

$$
\bar{H}_d = \left[\begin{array}{c} 0_{m_c \times n} \\ \hline H_d \end{array}\right].
$$

Starting from any initial guess matrix $H_{c,d} \in \mathscr{H}_{c,d}$, the gradient flow defined in (22) remains in the sub–set $\mathscr{H}_{c,d}$ and, on the basis of Theorem 1, it converges toward a hybrid measurement matrix, (locally) minimizing the squared Frobenius norm of the *a posteriori* covariance matrix. Multi–start strategies have to be used to circumvent the problem of local minima.

When noise is not negligible, without constraining the solution in $\mathscr{H}_{c,d}$ by W, the gradient search method of (22) would tend to produce measurement matrices whose continuous parts, H_c, are very large in norm. This is an obvious consequence of the fact that, for a fixed noise covariance R, larger measurement matrices H would produce an apparently higher signal–to–noise ratio in (1).

4.5 Continuous and Discrete Sensing Optimal Distribution

Results we have described in the past Sections show that, in case of continuous sensing design, the optimal choice H_c^* of the measurement matrix $H \in \mathbb{R}^{m \times n}$ is given by the first m principal components of the *a priori* covariance matrix P_o. Figure 5 shows the hand sensor distribution for a number $m = 1, 2, 3$ of noise-free measures (for lack of space we have reported only the continuous case).

In case of discrete sensing, H_d^* does not have an incremental behaviour, especially in case of few measures. In other words, the set of DoFs which have to be chosen in case of m measures does not necessarily contain all the set of DoFs chosen for $m - 1$ measures (for further details the reader is invited to refer to [3]).
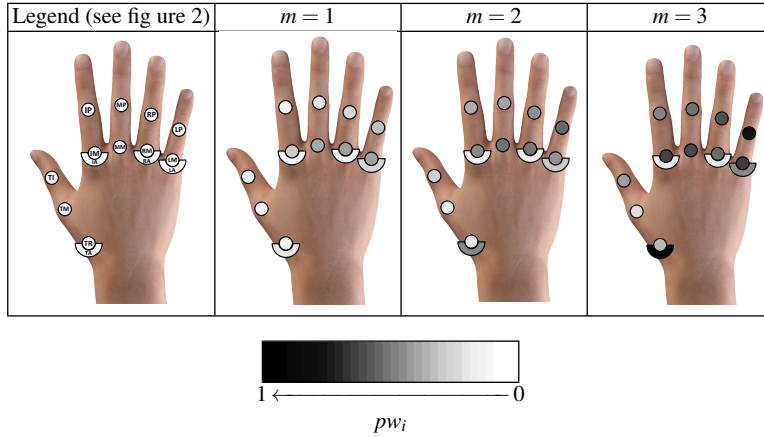
Fig. 5 Optimal continuous sensing distribution for $m = 1$, i.e. the first PC of P_o, for $m = 2$, i.e. the first two PCs of P_o and for $m = 3$, i.e. the first three PCs of P_o. The greater is the weight pw_i of the joint angle in the optimal measures, the darker is the color of that joint. I assume the weight of the i-th joint in the optimal measures given as $pw_i = \sum_{k=1}^{m} |h_{k,i}|$, where $h_{k,i}$ is the $(k,i)^{th}$ entry of matrix H, normalized w.r.t. the maximum value of pw_i. For example, for $m = 3$, weight of LA joint is 0.53, whereas for LM joint is 0.74 and the maximum value is for TA joint.
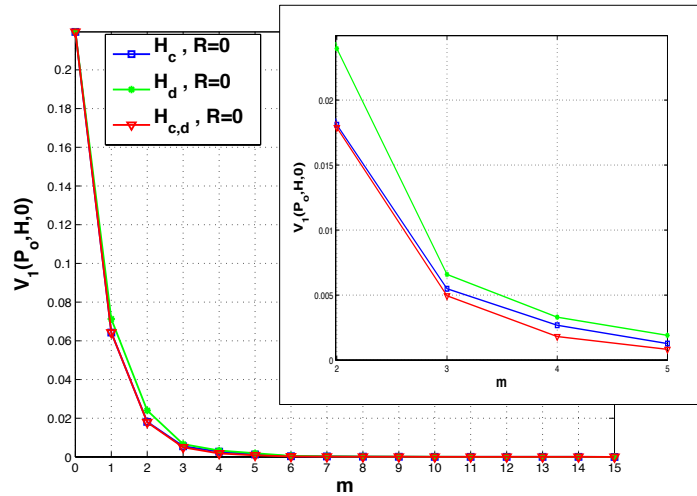

Fig. 6 Squared Frobenius norm of the *a posteriori* covariance matrix with noise–free measures in case of H_c^*, H_d^* and $H_{c,d}^*$ ($m_c = 1$) with an increasing number of noise-free measures. A zoomed detail of the graph is shown for $m = 2, 3, 4, 5$ measures.

Figure 6 shows the values of the squared norm of the *a posteriori* covariance matrix for increasing number m of measures. In particular, in figure 6 values of V_1 for matrices H_c^* and H_d^* are reported, for noise-free measures.

By analyzing how much V_1 reduces with the number of measurements w.r.t. the value it assumes for zero measures ($P_p \equiv P_0$), two types of observations can be done. First, the observed information quantified through V_1 (squared Frobenius norm of the *a posteriori* covariance matrix) is greatest for continuous case, while hybrid case provides better performance than the discrete one. Second, for the continuous case with noise–free measures, what is noticeable from the *observability* viewpoint is that a reduced number of measures coinciding with the first three principal components enable for $\simeq 97\%$ reduction of the squared Frobenius norm of the *a posteriori* covariance matrix. An analogous result can be found also under the *controllability* point of view. In [29] authors state that three postural synergies are crucial in grasp pre–shaping since they take into account for $\simeq 90\%$ of pose variability in grasping tasks.

4.6 Estimation Results with Optimal Discrete Sensing Devices

In this section, we compare the hand posture reconstruction obtained by H_s (which measured the joints (*TM*, *IM*, *MM*, *RM* and *LM*) with the one obtained by using the optimal matrix H_d^* with the same number of measurements in case of noisy measures (*TA*, *MM*, *RP*, *LA* and *LM*), where an additional random noise was artificially added on each measure. A zero–mean, Gaussian noise with standard deviation 0.122 rad ($7°$) was chosen based on data about common technologies and tools used to measure hand joint positions [32], thus obtaining a noise covariance matrix $R \approx \mathrm{diag}(0.0149)$.

Measures were provided by grasp data from the *validation set*, where degrees of freedom to be measured were chosen on the basis of optimization procedure outcomes, while the entire pose was recorded to produce an accurate reference posture. In order to compare reconstruction performance achieved with H_s and H_d^* we used as evaluation indices the average pose estimation error and average estimation error for each estimated DoF. Maximum errors are also reported.

In case of noise, performance in terms of average absolute estimation pose errors ($[°]$) obtained with H_d^* is better than the one exhibited by H_s (5.96 ± 1.42 vs. 8.18 ± 2.70). Moreover, maximum pose error with H_d^* is the smallest ($9.30°$ vs. $15.35°$ observed with H_s). Statistical difference between results from H_s and H_d^* is found (p=0.001). In table 2 average absolute estimation error with standard deviations are reported for each DoF. Also in this case, for the estimated DoFs, performance with H_d^* is always better or not statistically different from the one referred to H_s. Maximum estimation errors with H_d^* are usually inferior to the ones obtained with H_s.
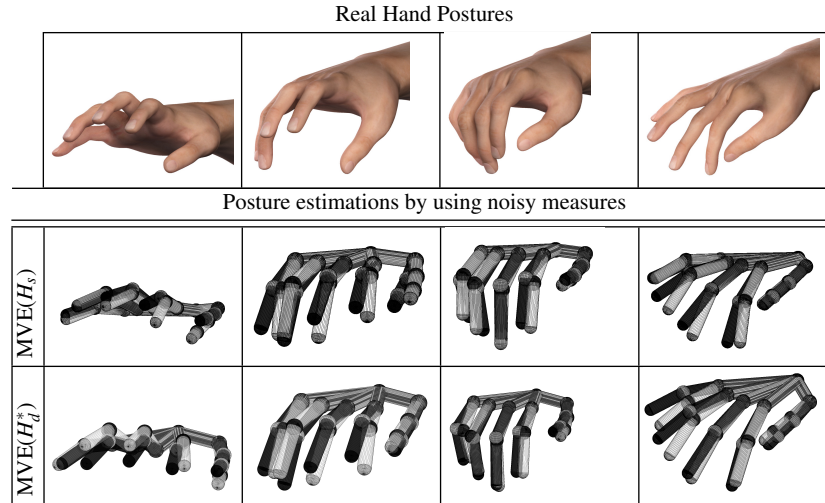
Real Hand Postures

Posture estimations by using noisy measures

Fig. 11 Hand pose reconstructions MVE algorithm by using matrix H_s which allows to measure TM, IM, MM, RM and LM and matrix H_d^* which allows to measure TA, MM, RP, LA and LM (see figure 2). In color the real hand posture whereas in white the estimated one.

5 Conclusions and Future Works

In this Chapter we have dealt with the problem of achieving reliable hand pose reconstructions through sensing gloves. More specifically, we have exploited the synergistic information on how humans use most frequently their hands to optimize estimation performance and optimally design sensing systems, when constraints on the number and quality of the sensors can limit measurement outcomes. Results show that the exploitation of *a priori* information on kinematic synergies can be profitably used to advance the state of art of sensing devices, offering new insights to further investigate the biology of human hand, e.g. in conjunction with the techniques described in Chapter 13, in a bi-directional inspiration and relationship between neuroscience and robotic/artificial systems.

Future works will aim at physically realizing an optimal sensing glove. We are considering different technological solutions, e.g. knitted piezoresistive fabrics (KPF) textile goniometer technology that was developed by coupling two piezoresistive layers through an electrically insulating middle layer [38]. Such a technology was already used to develop an under-sensed glove whose measurements were completed through synergistic information for functional grasp recognition [5].

The driving idea will be the synergy-based strategy described in this Chapter and protected by an Italian Patent [7], with the mid long-term of enabling mass production and commercialization for human-machine applications.

DoF	Mean Error [°]		H_s vs. H_d^*	Max Error [°]	
	H_s	H_d^*	p-values	H_s	H_d^*
TA$\otimes$	6.7±5.62	4.87±3.57	**0.19**	23.35	15.93
TR	7.65±5.57	7.54±5.00	**0.91** $\diamond$	27.46	22.73
TM$\circ$	2.81±1.75	2.63±1.90	**0.61** $\diamond$	7.2	8.78
TI	6.08±4.63	5.42±4.74	**0.32**	19.6	19.10
IA	10.74±5.6	11.52±5.81	**0.32**	27.31	28.46
IM$\circ$	4.15±3.17	6.91±5.00	0.003	11.66	21.49
IP	14.61±7.93	6.61±6.01	0	31.85	38.07
MM$\circ\otimes$	4.59±3.08	4.71±3.19	**0.77**	11.43	15.72
MP$\otimes$	13.71±8.07	4.08±2.98	0 ‡	37.61	13.71
RA	3.12±2.37	3.28±2.45	**0.71**	9.18	9.37
RM$\circ$	4.03±3.07	6.30±4.72	0.01 ‡	12.94	12.91
RP	16.78±11.07	6.89±3.82	0 ‡	50.66	16.34
LA	8.97±5.11	9.86±5.45	**0.38** $\diamond$	20.86	21.48
LM$\circ\otimes$	3.82±3.05	4.82±4.30	**0.44**	11.33	14.26
LP$\otimes$	14.64±9.68	3.94±2.95	0	48.61	11.03

1 $\leftarrow$ ———————————————————— $\rightarrow$ 0

p-values

$^\circ$ indicates a DoF measured with H_s
$^\otimes$ indicates a DoF measured with H_d^*

Table 2 Average estimation errors and standard deviation for each DoF [$\circ$] for the simulated acquisition considering H_s and H_d^* both with five noisy measures. Maximum errors are also reported as well as p-values from the evaluation of DoF estimation errors between H_s and H_d^*. $\diamond$ indicates T_{eq} test. ‡ indicates T_{neq} test. When no symbol appears near the tabulated values, U test is used. **Bold** value indicates no statistical difference between the two methods under analysis at 5% significance level. When the difference is significative, values are reported with a 10^{-4} precision. p-values less than 10^{-4} are considered equal to zero. Symbol "–" is used for those DoFs which are measured by both H_s and H_d^*. For further details on statistical tools, the reader is invited to refer to Table 1.

6 Acknowledgements

References

[1] Bianchi M, Salaris P, Bicchi A (2013) Synergy-based hand pose sensing: Optimal glove design. The International Journal of Robotics Research 32(4):407–424

[2] Bianchi M, Salaris P, Bicchi A (2013) Synergy-based hand pose sensing: Optimal glove design. The International Journal of Robotics Research 32(4):407–424

[3] Bianchi M, Salaris P, Bicchi A (2013) Synergy-based hand pose sensing: Reconstruction enhancement. International Journal of Robotics Research 32(4):396–406

[4] Bianchi M, Salaris P, Bicchi A (2013) Synergy-based hand pose sensing: Reconstruction enhancement. International Journal of Robotics Research 32(4):396–406

[5] Bianchi M, Carbonaro N, Battaglia E, Lorussi F, Bicchi A, De Rossi D, Tognetti A (2014) Exploiting hand kinematic synergies and wearable under-sensing for hand functional grasp recognition. In: Wireless Mobile Communication and Healthcare (Mobihealth), 2014 EAI 4th International Conference on, IEEE, pp 168–171

[6] Bicchi A, Canepa G (1994) Optimal design of multivariate sensors. Measurement Science and Technology (Institute of Physics Journal "E") 5:319–332

[7] Bicchi A, Bianchi M, Salaris P (2014) A method for optimal hand pose reconstruction. Patent, 0001410855

[8] Brown C, Asada H (2007) Inter-finger coordination and postural synergies in robot hands via mechanical implementation of principal component analysis. In: IEEE-RAS International Conference on Intelligent Robots and Systems, pp 2877 – 2882

[9] Catalano MG, Grioli G, Farnioli E, Serio A, Piazza C, Bicchi A (2014) Adaptive synergies for the design and control of the pisa/iit softhand. International Journal of Robotics Research 33:768–782, DOI 10.1177/0278364913518998

[10] Chaloner K, Verdinelli I (1995) Bayesian experimental design: A review. Statistical Science 10(3):273–304

[11] Diamantaras K, Hornik K (1993) Noisy principal component analysis. Measurement'93 pp 25 – 33

[12] Dipietro L, Sabatini AM, Dario P (2008) A survey of glove-based systems and their applications. Systems, Man, and Cybernetics, Part C: Applications and Reviews, IEEE Transactions on 38(4):461 –482

[13] Edin BB, Abbs JH (1991) Finger movement responses of cutaneous mechanoreceptors in the dorsal skin of the human hand. Journal of Neurophysiology 65(3):657–670

[14] Edin BB, Abbs JH (1991) Finger movement responses of cutaneous mechanoreceptors in the dorsal skin of the human hand. J Neurophysiology 65(3):657–670

[15] Fahrer M (1981) The hand, Philadelphia, PA: Saunders, chap Interdependent and independent actions of the fingers, pp 399 – 403

[16] Fu Q, Santello M (2010) Tracking whole hand kinematics using extended kalman filter. In: Engineering in Medicine and Biology Society (EMBC), 2010 Annual International Conference of the IEEE, pp 4606 – 4609

[17] Gabiccini M, Bicchi A (2010) On the role of hand synergies in the optimal choice of grasping forces. In: Robotics Science and Systems

[18] Gabiccini M, Stillfried G, Marino H, Bianchi M (2013) A data-driven kinematic model of the human hand with soft-tissue artifact compensation mechanism for grasp synergy analysis. In: Intelligent Robots and Systems (IROS), 2013 IEEE/RSJ International Conference on, pp 3738–3745, DOI 10.1109/IROS.2013.6696890

[19] Gelb A (1974) Applied Optimal Estimation. M.I.T. Press, Cambridge, US-MA

[20] Ghosh S, Rao CR (1996) Review of optimal bayes designs. In: Design and Analysis of Experiments, Handbook of Statistics, vol 13, Elsevier, pp 1099 – 1147

[21] Hawkins DM (1980) Identification of Outliers. Chapman and Hall, London

[22] Kilbreath SL, Gandevia SC (2002) Limited independent flexion of the thumb and fingers in human subjects. J Physiol 543:289 – 296

[23] Lorussi F, Rocchia W, Scilingo EP, Tognetti A, De Rossi DE (2004) Wearable, redundant fabric-based sensor arrays for reconstruction of body segment posture. Sensors Journal, IEEE 4(6):807 – 818

[24] Mahalanobis PC (1936) On the generalised distance in statistics. Proceedings of the National Institute of Sciences of India 2(1):49 – 55

[25] Mason CR, Gomez JE, Ebner TJ (2001) Hand synergies during reach-to-grasp. J Neurophysiol 86:2896 – 2910

[26] Mulatto S, Formaglio A, Malvezzi M, Prattichizzo D (2010) Animating a synergy-based deformable hand avatar for haptic grasping. In: International Conference EuroHaptics, vol 2, pp 203–210

[27] Rao CR (1964) The use and interpretation of principal component analysis in applied research. The Indian journal of statistic

[28] Rosen JB (1960) The gradient projection method for nonlinear programming. part i. linear constraints. Journal of the Society for Industrial and Applied Mathematics 8(1):181 – 217

[29] Santello M, Flanders M, Soechting JF (1998) Postural hand synergies for tool use. The Journal of Neuroscience 18(23):10,105 – 10,115

[30] Santello M, Baud-Bovy G, Jörntell H (2013) Neural bases of hand synergies. Frontiers in computational neuroscience 7

[31] Schieber MH, Santello M (2004) Hand function: peripheral and central constraints on performance. Journal of Applied Physiology 96(6):2293 – 2300

[32] Simone LK, Sundarrajan N, Luo X, Jia Y, Kamper DG (2007) A low cost instrumented glove for extended monitoring and functional hand assessment. Journal of Neuroscience Methods 160(2):335–348

[33] Stillfried G, van der Smagt P (2010) Movement model of a human hand based on magnetic resonance imaging (mri). In: Proc. ICABB

[34] Sturman DJ, Zeltzer D (1994) A survey of glove-based input. Computer Graphics and Applications, IEEE 14(1):30–39

[35] Tarantola A (2005) Inverse Problem Theory and Model Parameter Estimation. SIAM

[36] Tognetti A, Carbonaro N, Zupone G, De Rossi DE (2006) Characterization of a novel data glove based on textile integrated sensors. In: Annual Interna-

tional Conference of the IEEE Engineering in Medicine and Biology Society, EMBC06, Proceedings., pp 2510 – 2513

[37] Tognetti A, Carbonaro N, Dalle Mura G, Tesconi M, Zupone G, De Rossi DE (2008) Sensing garments for body posture and gesture classification. TECH-NICAL USAGE TEXTILES Magazine 68:33–39

[38] Tognetti A, Lorussi F, Mura G, Carbonaro N, Pacelli M, Paradiso R, Rossi D (2014) New generation of wearable goniometers for motion capture systems. Journal of neuroengineering and rehabilitation 11(1):56

[39] Zavlanos MM, Pappas GJ (2006) A dynamical systems approach to weighted graph matching. In: Decision and Control, 2006 45th IEEE Conference on, pp 3492 – 3497

[40] Zhang X, Lee S, Braido P (2003) Determining finger segmental centers of rotation in flexion-extension based on surface marker measurement. Journal of Biomechanics 36:1097 – 1102